JOURNAL OF MATERIALS SCIENCE 31 (1996) 6495–6500

Variations in microstructure and composition of indium tin oxide films with the deposition technique

M. ROTTMANN*, H. HENNIG, B. ZIEMER, R. KALÄHNE, K. H. HECKNER
Humboldt-Universität zu Berlin, Institut für Physikalische und Theoretische Chemie, D-10117 Berlin, Bunsenstraße 1, Germany

Indium tin oxide (ITO) films have been deposited by reactive d.c.-sputtering and also by the reactive thermal evaporation technique onto glass substrates. The relationship between the microstructure and composition of the ITO films was found to strongly depend on the deposition technique. In addition the application of pure water vapour as the reactive sputtering atmosphere and its influence on the structural and compositional properties of the ITO films has been studied.

X-ray diffraction investigations showed that all the films exhibited the bixbite structure of In_2O_3. No other crystalline phases were observed. Highly crystallized ITO films have been obtained using the reactive thermal evaporation technique. These films show a large average grain size of about 80 nm and a very homogeneous morphology. In contrast the d.c.-sputtered ITO films have a smaller average grain size and a characteristic texture. All deposited ITO films show an enlarged lattice constant compared to that of In_2O_3. A strong dependence of the chemical composition of the ITO films on the deposition technique and parameters was detected.

1. Introduction

Indium tin oxide (ITO) films find use in a wide range of applications due to their highly conductive and transparent nature. The high conductance is generated by a high doping level of Sn dopants and oxygen vacancies in the In_2O_3 lattice. Due to a high energy band gap, $E_g = 3.65$ eV [1–3], ITO appears highly transparent in visible wavelengths. These optical and electrical properties make ITO films useful for various applications, e.g., transparent electrodes in liquid crystal displays solar cells, detectors and as a transparent heat reflecting window material. Many techniques such as evaporation, sputtering, chemical vapour deposition and spraying methods have been employed to deposit thin ITO films on several substrates.

The ITO films exhibit in most cases the bixbite [$(Mn, Fe)_2O_3$] structure of In_2O_3. However, depending on the exact deposition conditions the ITO films can show strong variations in their morphology and crystallographic properties (e.g., texture, grain size, lattice constant). In this paper intensive studies on the structural and compositional properties of ITO films are reported. ITO films deposited by reactive d.c.-sputtering and reactive thermal evaporation were characterized and their properties correlated with the different deposition techniques. During sputtering and evaporation pure O_2 was used as the reactive atmosphere. In addition we tested the use of pure water vapour as the reactive sputtering atmosphere and investigated its influence on the crystallographic properties of the deposited films.

2. Experimental procedure

The ITO films were deposited by (a) the reactive d.c. sputtering deposition technique and (b) the reactive thermal evaporation technique onto cleaned glass (Corning glass 0317) substrates.

The d.c. sputtering deposition was carried out with the sputtering system A 550 VZK (Leibold-Heraeus). An In–Sn-alloy target (In:Sn = 80:20 wt %) and both pure O_2 and water vapour [6, 7] were used as the reactive sputtering gas. During the sputtering process the following deposition parameters were kept constant: d.c. voltage: 2.6 kV, sputtering current: 0.9 A, substrate temperature: 350 °C and O_2-pressure: 4 Pa, H_2O-pressure: 10Pa. For further details see reference [4].

Thermal evaporation growth of ITO films was performed in a vacuum deposition system, B30 (Hochvakuum Dresden). An In–Sn alloy (made of 99.999% purity metals, In:Sn = 90:10 wt %) was evaporated from a tungsten boat in the presence of oxygen. The purified glass substrates were kept at a distance of 15 cm above the source. Prior to deposition the system was evacuated up to a pressure of 1×10^{-3} Pa. During the deposition pure oxygen was allowed into the evaporation chamber up to a pressure of 10 Pa.

**Present address*: Siemens Matsushita Components, OFW FP PT, Postfach 80 17 09, 81617 München, Germany.

0022–2461

The deposition rate was controlled by an oscillation quartz crystal and regulated between 0.2–0.3 nm per s. Substrate temperatures in the range of 340–355 °C were achieved by resistance heating which was controlled with a Cr–Ni thermocouple.

Film thickness measurements were made using a 'Talystep' profile tester (Rank Taylor Hobson Co.). The chemical composition of the ITO films was analysed by atomic emission spectroscopy (ICP-AES) using a Unicam 701 AES spectrometer. Data were collected after the ITO films had been completely dissolved in 4 N HCl. X-ray diffraction analyses were performed with a powder diffractometer model HZG 4 (Freiberger Präzisionsmechanik) using Cu-K_α radiation with $\lambda = 0.15418$ nm. Raster electron microscopy (REM) investigations were carried out with a REM microscope, Alpha 9 (Akashi). The films were covered with a 20 nm sputtered gold layer before the measurements were performed.

3. Results and discussion

3.1. Structural characterization

The microstructure of deposited ITO films were analysed by X-ray diffraction (XRD). We show XRD patterns of the d.c. sputtered and thermally evaporated ITO films in Figs 1–3. The peaks observed in the XRD pattern match with In_2O_3 peaks in accordance with the JCPDS powder diffraction file of In_2O_3, PDF 6-416. No other crystalline phases were observed.

There are significant differences between the investigated ITO films. Whereas d.c.-O_2-sputtered (Fig. 1) and thermally evaporated ITO films (Fig. 3) show the most intense peaks of In_2O_3: ⟨222⟩, ⟨440⟩ and ⟨400⟩, the ⟨400⟩ peak disappears in the XRD pattern of d.c.-H_2O-sputtered ITO-films (Fig. 2). It is observed that these peaks have different intensities depending on the growth techniques. The reflections of the d.c.-O_2-sputtered ITO film (Fig. 1) show relatively low intensities compared to those of the other films. Using H_2O as the reactive sputtering gas produces ITO films that show a very strong dominating ⟨222⟩ peak in the X-ray diffraction pattern (Fig. 2). It has more than 50 times the intensity of the other observed peaks. We will focus our discussion on the

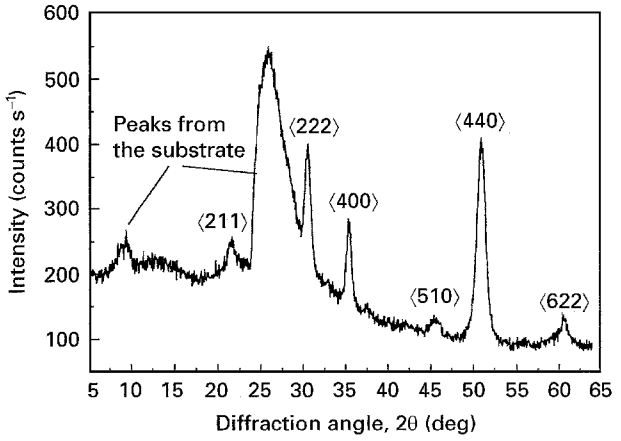

Figure 1 X-ray diffraction pattern of a d.c.-O_2-sputtered ITO film, film thickness 440 nm.

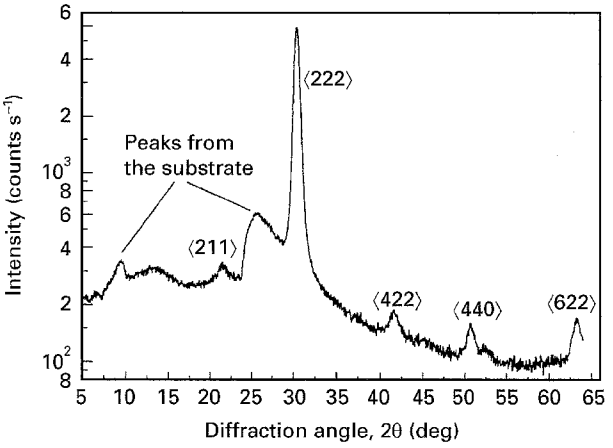

Figure 2 X-ray diffraction pattern of a d.c.-H_2O-sputtered ITO film, film thickness 365 nm.

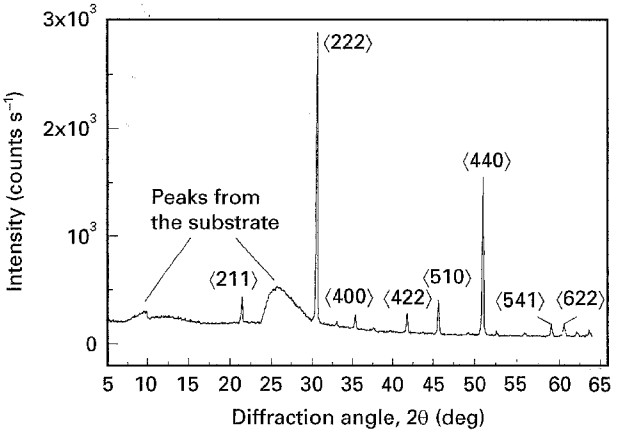

Figure 3 X-ray diffraction pattern of a thermally evaporated ITO film, film thickness 210 nm.

3 most important peaks of In_2O_3 namely the ⟨222⟩, ⟨400⟩ and ⟨440⟩ reflections. These peaks for the ITO films are shown in expanded form in Figs 4–6. Significant differences in intensity, diffraction angle and half peak width of these reflections are clearly observable. Table 1 shows that the intensities of the ⟨222⟩, ⟨400⟩ and ⟨440⟩ reflections of the ITO films deviate from the PDF intensities. This implies that the particles in the ITO films are not arranged statistically in the oxide layer instead they are arranged in a preferred orientation. The d.c.-O_2-sputtered ITO films show a ⟨110⟩ texture because of an increased intensity of the ⟨440⟩ reflections compared to In_2O_3 (PDF 6-416). Due to the very intensive ⟨222⟩ peak d.c.-H_2O-sputtered ITO films exhibit a strong ⟨111⟩ texture. This is caused by a preferred orientation of particles in the ⟨111⟩ direction which results in improved optical and electrical properties [4, 5]. Thermally evaporated ITO films exhibit two characteristic textures: the ⟨111⟩ and the ⟨110⟩ texture. When textured ITO films are produced they often show the ⟨111⟩ preferred orientation [3, 8–14] but sometimes the ⟨110⟩ [13] and the ⟨100⟩ texture [15] have been observed. A correlation of the observed texture to deposition technique is not yet possible.

TABLE I Relative intensities of XRD reflections of ITO films compared to In_2O_3 (PDF 6-416)

	In_2O_3	d.c.-O_2-sputtered ITO	d.c.-H_2O-sputterd ITO	Thermally evaporated ITO
hkl	Intensity (%)	Intensity (%)	Intensity (%)	Intensity (%)
222	100	66	100	100
400	30	34	–	3
440	35	100	1	53

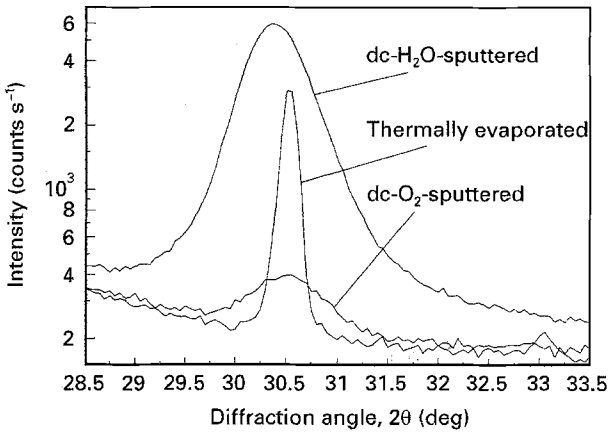

Figure 4 Expanded ⟨222⟩ peaks of d.c.-O_2-sputtered, d.c.-H_2O-sputtered and thermally evaporated ITO films.

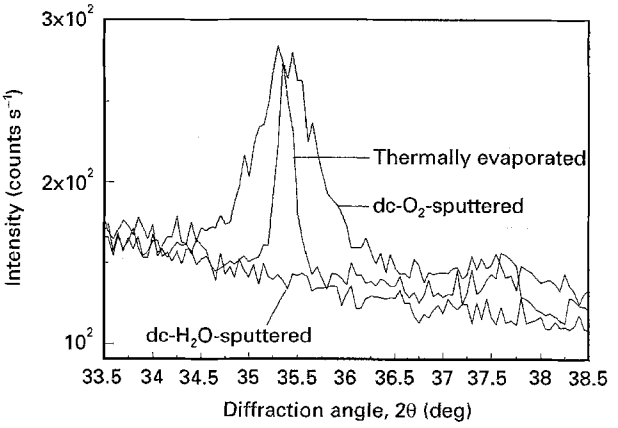

Figure 6 Expanded ⟨400⟩ peaks of d.c.-O_2-sputtered, d.c.-H_2O-sputtered and thermally evaporated ITO films.

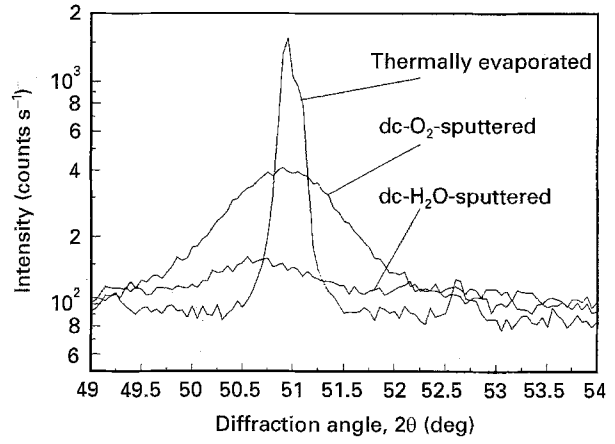

Figure 5 Expanded ⟨440⟩ peaks of d.c.-O_2-sputtered, d.c.-H_2O-sputtered and thermally evaporated ITO films.

The lattice parameters for cubic systems can be calculated from Equations 1 and 2. The data analysis results are summarized in Table II.

$$2d \sin\theta = n\lambda \tag{1}$$

$$\frac{n^2}{d^2} = \frac{(h^2 + k^2 + l^2)}{a^2} \tag{2}$$

$$r = \frac{\lambda}{\Delta\Theta \cdot \cos\Theta} \tag{3}$$

where θ is the angle of reflection; λ is the wavelength of Cu-K_α X-ray radiation; d is the distance of net planes; n is the order of interference; h, k, l are the Miller indices; a is the lattice constant; $\Delta\Theta$ is the half peak width and r is the size of crystallites

The lattice parameters of all ITO films are higher than the value for undoped In_2O_3 which indicates an occupation of interstitial sites by dopants [16]. A very large enhancement in the value of the lattice parameters is shown in d.c.-H_2O-sputtered ITO films.

An estimation of the average grain size in the ITO films is possible using the Laue–Scherrer formula shown in Equation 3. For the ⟨222⟩, ⟨440⟩ and ⟨400⟩ directions the calculated grain sizes of ITO films are given in Table III. The largest particle size of about 80 nm occurs in the thermally evaporated ITO films that are highly crystallized. Smaller average grain sizes are observed for the d.c. sputtered ITO films. We determined an average grain size of $r = 23$ nm for d.c.-O_2-sputtered and $r = 33$ nm d.c.-H_2O-sputtered ITO. The grain sizes vary with the different plane directions. Thermal evaporated and d.c.-O_2-sputtered ITO films show an especially large grain size in the ⟨100⟩ direction. This has also been observed by Parent *et al.* [15]. In d.c.-H_2O-sputtered ITO films the ⟨400⟩ reflection is not observed and thus, thereby in this case the maximum grain size occurs in the ⟨110⟩ direction.

The reason for the smaller average grain sizes in the d.c. sputtered ITO films compared to thermally evaporated films is to be found in the deposition process. During the d.c. sputtering procedure a bombardment of the substrate and the growing ITO film with high energy particles ($E \approx 100$–1000 eV) takes place [17]. This causes surface damage and leads to a disturbance

TABLE II Calculated lattice constants of ITO films in relation to undoped In_2O_3. The value of the lattice constant for In_2O_3 is taken from PDF6-416

	In_2O_3	d.c.-O_2-sputtered ITO	d.c.-H_2O-sputterd ITO	Thermally evaporated ITO
hkl	a (nm)	a (nm)	a (nm)	a (nm)
222	1.0118	1.0142	1.0185	1.0136
400	1.0118	1.0142	–	1.0142
440	1.0118	1.0136	1.0174	1.0128
∅	1.0118	1.0140	1.0180	1.0135

TABLE III Grain size of ITO films in the ⟨222⟩, ⟨400⟩ and ⟨440⟩ directions, calculated according Laue–Scherrer equation

	d.c.-O_2-sputtered ITO film	d.c.-H_2O-sputtered ITO film	Thermally evaporated ITO film
hkl	r (nm)	r (nm)	r (nm)
222	21	27	70
400	32	–	83
440	17	40	68
∅	23	34	74

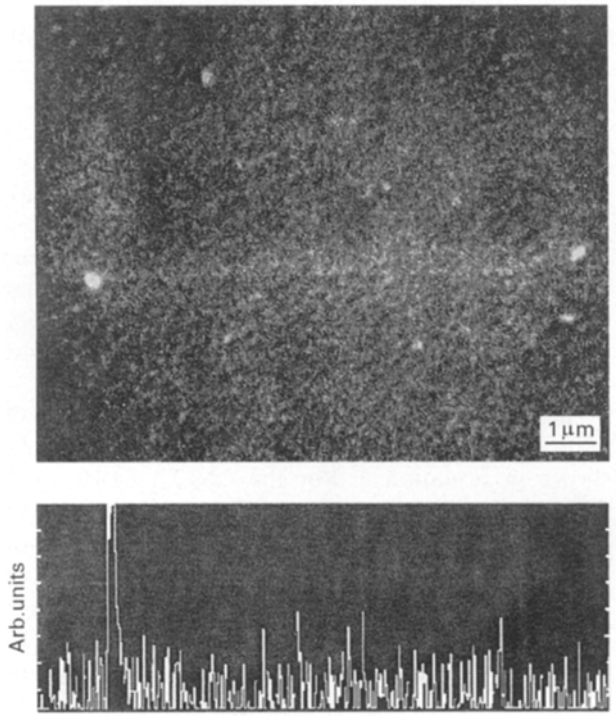

Figure 7 REM photograph of a d.c.-O_2-sputtered ITO film, film thickness 440 nm.

of the crystal growth. During thermal evaporation the liberated particles have only a small kinetic energy (0.1 eV) [17], and thus larger crystals arise in the ITO film.

The REM images and surface profiles of the ITO films are shown in Figs 7–9. For a d.c.-O_2-sputtered ITO film the grain size estimated from Fig. 7 agrees with that calculated previously. The use of H_2O vapour as the reactive sputtering gas changes the morphology of the ITO films drastically. The REM image and the surface profile (Fig. 8) show a very homogeneous surface without the appearance of a characteristic particle pattern. The large grain size of thermally evaporated ITO films is confirmed by the REM photograph and its surface profile.

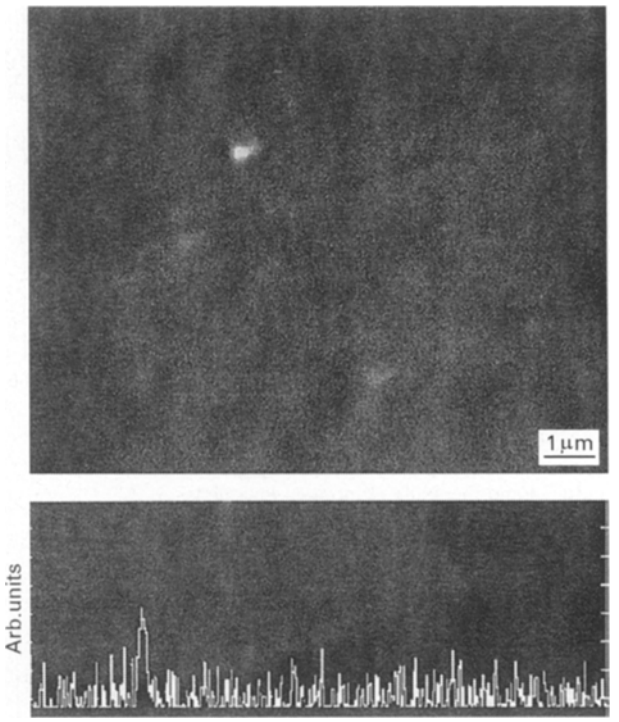

Figure 8 REM photograph of a d.c.-H_2O-sputtered ITO film, film thickness 365 nm.

3.2. Chemical composition of the ITO films

Table IV shows the analysed In:Sn ratios of the source alloy and the deposited ITO films. There are great differences between the source and ITO films. The d.c.-O_2-sputtered ITO films exhibit an enrichment of In in the film compared to the sputtering target. In contrast, we observed an increase of Sn in the d.c.-H_2O-sputterd ITO films up to an In:Sn ratio of 75/25. A very small tin concentration of only 1% was analysed for the thermally evaporated ITO films.

In both types of sputter deposition the tin concentrations in the ITO films differ from the tin concentration of the sputtering target, which was also observed by Takaki *et al.* [14]. For sputtering in pure H_2O, it is assumed that the target surface is completely covered with $In(OH)_3$ and $Sn(OH)_x$ ($x = 2$ or 4). Because of the

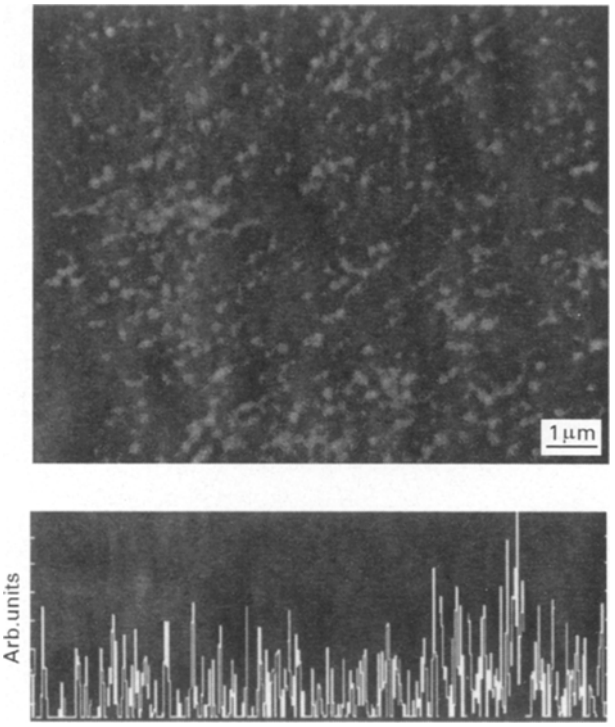

Figure 9 REM photograph of a thermally evaporated ITO film, film thickness 210 nm.

TABLE IV In:Sn-ratio of the deposited ITO films and the source material

Sample	In:Sn (wt %)	In:Sn of source alloy (wt %)
d.c.-O_2-ITO	85:15	80:20
d.c.-H_2O-ITO	76:24	80:20
Thermally evaporated ITO	99:1	90:10

higher volatility of tin hydroxide relative to indium hydroxide the Sn hydroxide will be preferentially sputtered from the target. This results in a higher sputtering rate of tin and a higher tin concentration in the ITO film. Sputtering in pure O_2 produces a thin film of In_2O_3 and SnO_2 on the target surface. In_2O_3 exhibits a higher volatility than SnO_2, leading to a higher sputtering rate of In and an enrichment of it in the ITO film.

The very small tin concentrations in the thermally evaporated ITO films as compared to the evaporation alloy has also been observed by Jan and Lee [18]. Since In has a higher vapour pressure than Sn, it will be preferently vapourized. This will change the vapour composition which leads to a strong enrichment of In in the thermally evaporated ITO films.

Now a direct correlation between the dopant concentrations and the lattice parameter of the ITO films is possible. At implantation of Sn in In_2O_3 only Sn^{4+} ions are detected [19]. Although the ionic radius of Sn^{4+} (0.071 nm) is smaller than the ionic radius of In^{3+} (0.081 nm) an expansion of the In_2O_3 lattice is observed. This indicates that a part of Sn-dopants occupy interstitial sites.

4. Conclusions

The structural and compositional characteristics for reactively deposited ITO films have been clarified. The ITO films were deposited on to glass substrates by reactive d.c. sputter deposition using (a) pure O_2 and (b) water vapour as the reactive sputtering atmosphere and also by thermal evaporation. The investigated ITO films exhibit the following common features.

All investigated ITO films crystallize in the structure of In_2O_3. They are polycrystalline and show characteristic textures. The doping with tin causes an expansion of In_2O_3 host lattice which is reflected in an increase of the lattice parameters. This can be explained by an occupation of interstitial sites in the In_2O_3 lattice by tin. The ITO films have tin concentration which differs from the source In–Sn alloy.

The differences are the following.

The XRD pattern shows a $\langle 1\,1\,0\rangle$ texture for d.c.-O_2-sputtered, a strong $\langle 1\,1\,1\rangle$ texture for d.c.-H_2O-sputtered and both a $\langle 1\,1\,1\rangle$ as well as a $\langle 1\,1\,0\rangle$ texture for thermally evaporated ITO films. By application of the reactive thermal evaporation technique highly crystallized ITO films are obtained. Inspite of a layer thickness of only 210 nm, very large particles with an average grain size of about 77 nm are observed. Because of a pronounced preferred orientation of particles in the $\langle 1\,1\,1\rangle$ direction observed in REM photographs d.c.-H_2O-sputtered ITO films show a very homogeneous surface.

The application of H_2O vapour as the reactive sputtering gas produces ITO films that are distinguished by a high tin concentration. This causes a high electrical conductance [5]. Only a very small tin concentration was obtained in ITO films grown by the thermal evaporation deposition technique.

References

1. Y. OHHATA, F. SHINOKI and S. YOSHIDA, *Thin Solid Films* **59** (1979) 255.
2. L. GUPTA, A. MANSINGH and P. K. SRIVASTAVA, *ibid.* **176** (1989) 33.
3. N. BALASUBRAMANIAN and A. SUBRAMAMANYAM, *J. Phys. D: Appl Phys.* **22** (1989) 206.
4. M. ROTTMANN and K. H. HECKNER, *Proc. SPIE* **2255** (1994) 628.
5. *Idem., J. Phys. D: Appl. Phys.* **28** (1995) 1448.
6. M. ROTTMANN, A. HERBST and K. H. HECKNER, Ger. Offen. DE 4, 126, 812 (Cl.C23C14/34) 11. Febr. 1993, Appl. 09. Aug. 1991 (1993).
7. *idem.*, Ger. Offen. DE 4, 126, 811 (Cl.C23C14/08) 11. Febr. 1993, Appl. 09. Aug. 1991 (1993).
8. J. C. C. FAN and F. J. BACHNER, *J. Electrochem. Soc.* **122** (1975) 1719.
9. P. J. MARTIN and R. P. NETTERFIELD, *Thin Solid Films* **207** (1986) 137.
10. P. NATH, R. F. BUNSHAH, B. M. BASOL and O. M. STAFFSUD, *ibid.* **72** (1980) 463.
11. T. SUZUKI, T. YAMAZAKI and H. ODA, *J. Mater. Sci.* **23** (1988) 3026.
12. T. SUZUKI, T. YAMAZAKI, M. TAKIZAWA and O. KAWASAKI, *ibid.* **24** (1989) 187.
13. M. HIGUCHI, M. SAWADA and Y. KURONUMA, *J. Electrochem. Soc.* **140** (1993) 1773.
14. S. TAKAKI, K. MATSUMOTO and K. SUZUKI, *Appl. Surf. Sci.* **33/34** (1988) 919.

15. P. PARENT, H. DEXPERT, G. TOURILLON and J. M. GRIMAL, *J. Electrochem. Soc.* **139** (1992) 276.
16. Y. SHIGESATO, S. TAKAKI and T. HARANOU, *Appl. Surf. Sci.* **48/49** (1991) 269.
17. B. ROTHER and J. VETTER, "Plasma- Beschichtungsverfahren und Hartstoffschichten" (Deutscher Verlag für Grundstoffindustrie, Leipzig, 1992)
18. S. W. JAN and S. C. LEE, *J. Electrochem. Soc.* **134** (1987) 2056.
19. J. KANAZAWA, T. HARANOH and K. MATSUMOTO, *Vacuum* **41** (1990) 1463.

Received 15 September 1995
and accepted 15 January 1996